의학석사 학위논문

Anti-inflammatory Effects of *Allium cepa* L. Peel Extracts on the JAK-STAT Pathway Inhibition in LPS-stimulated RAW264.7 Cells

대식세포에서 *Allium cepa* L. 껍질 추출물의 JAK-STAT 경로 억제를 통한 항염증 효능에 관한 연구

2023년 8월

서울대학교 대학원
의과학과 의과학전공
이 현 승

A thesis of the Degree of Master of Philosophy

Anti-inflammatory Effects of *Allium cepa* L. Peel Extracts on the JAK-STAT Pathway Inhibition in LPS-stimulated RAW264.7 Cells

대식세포에서 *Allium cepa* L. 껍질 추출물의
JAK-STAT 경로 억제를 통한
항염증 효능에 관한 연구

August 2023

The Department of Biomedical Sciences,
(Major in Biomedical Sciences)
Seoul National University
College of Medicine

Hyun-Seung Lee

대식세포에서 *Allium cepa* L. 껍질 추출물의 JAK-STAT 경로 억제를 통한 항염증 효능에 관한 연구

지도 교수 예 상 규

이 논문을 의학석사 학위논문으로 제출함
2023년 4월

서울대학교 대학원
의과학과 의과학전공
이 현 승

이현승의 의학석사 학위논문을 인준함
2023년 7월

위 원 장 _____ (인)

부위원장 _____ (인)

위 원 _____ (인)

Anti-inflammatory Effects of *Allium cepa* L. Peel Extracts on the JAK-STAT Pathway Inhibition in LPS-stimulated RAW264.7 Cells

by

Hyun-Seung Lee

A thesis submitted to the Department of Biomedical Sciences in partial fulfillment of the requirements for the Degree of Master of Philosophy in Biomedical Sciences at Seoul National University College of Medicine

July 2023

Approved by Thesis Committee:

Chair _____**(Seal)**

Vice Chair _____**(Seal)**

Examiner _____**(Seal)**

ABSTRACT

Allium cepa L. (*A. cepa*) is one of the oldest cultivated plants in the world. It is used in food and medicine and is known to relieve inflammatory diseases. *A. cepa* peel has a higher content of flavonoids, such as quercetin, than the edible parts. These flavonoids alleviate inflammatory diseases. However, the anti-inflammatory effects of *A. cepa* peel extracts obtained using various extraction methods and their underlying detailed mechanisms require further investigation.

The present study aimed to observe the anti-inflammatory effects of the *A. cepa* peel extracts obtained using various extraction methods and the related detailed mechanisms of *A. cepa* peel extracts in lipopolysaccharide (LPS)-induced RAW264.7 cells. Of the three *A. cepa* peel extracts obtained using different extraction methods, the *A. cepa* peel 50% EtOH extract (AP50E) was the most effective at inhibiting LPS-induced nitric oxide (NO) and inducible nitric oxide synthase (iNOS). Furthermore, AP50E significantly reduced the levels of pro-inflammation cytokines interleukin (IL)-1α, IL-1β, IL-6, and IL-27. Additionally, AP50E directly inhibited the Janus kinase-signaling transducer and activator of transcription (JAK-STAT) pathway.

These results showed that AP50E exhibited an anti-inflammatory effect in LPS-induced RAW264.7 mouse macrophages by directly inhibiting JAK-

STAT signaling. Based on these findings, I propose AP50E as a potential candidate for the development of preventive or therapeutic agents against inflammatory diseases.

Keywords: *Allium cepa* L., macrophage, anti-inflammatory effects, Janus kinase (JAK), Signaling transducer and activator of transcription (STAT)

Student Number: 2021-22420

CONTENTS

LIST OF FIGURES AND TABLES

LIST OF ABBREVIATIONS

***A. cepa*:** *Allium cepa* L.

APW: *A. cepa* peel hot water extract

AP30E: *A. cepa* peel 30% EtOH extract

AP50E: *A. cepa* peel 50% EtOH extract

CM: Conditioned medium

DMSO: Dimethyl sulfoxide

DMEM: Dulbecco's Modified Eagle's Medium

ELISA: Enzyme-linked immunosorbent assay

EtOH: Ethanol

FBS: Fetal bovine serum

HRP: Horseradish peroxidase

iNOS: Inducible nitric oxide synthase

IL: Interleukin

JAK: Janus kinase

LPS: Lipopolysaccharide

MAPK: Mitogen-activated protein kinase

MTT: 3-(4,5-dimethylthiazol-2-yl)-2,5-diphenyltetrazolium bromide

MYD88: Myeloid differentiation primary response 88

NO: Nitric oxide

NF-κB: Nuclear factor kappa-light-chain-enhancer of activated B cells

PBS: Phosphate buffered saline

RT-qPCR: Quantitative reverse transcription polymerase chain reaction

SDS: Sodium dodecyl sulfate

STAT: Signaling transducer and activator of transcription

TLR: Toll-like receptor

TNF-α: Tumor necrosis factor-α

INTRODUCTION

Inflammation is an important defense mechanism in living organisms against harmful stimuli such as pathogens and irritants [1]. Acute and controlled inflammation is a protective immune response that eliminates injurious external stimuli, facilitates healing, and maintains homeostasis of tissues and organs [2]. However, prolonged and uncontrolled inflammation can lead to chronic diseases such as cardiovascular disease, rheumatoid arthritis, autoimmune disease, neurological disease, and cancer [3]. Therefore, it is important to identify treatment strategies that suppress excessive inflammatory responses.

Macrophages differentiate from blood monocytes and play a protective role in the inflammatory response [4]. Toll-like receptor 4 (TLR4), expressed on the macrophage membrane, is stimulated by LPS derived from the gram-negative bacteria, and the stimulated TLR4 activates downstream signal like mitogen activated protein kinases (MAPKs) and nuclear factor (NF)-κB [5]. Through this signaling pathway, the expression of iNOS, an NO synthase, is increased which leads to NO production which in excess causes excessive inflammation (Sharma et al., 2007).

JAK-STAT signaling is an important inflammatory signaling pathway that mediates the immune response [6]. In macrophages, the LPS-induced increase in inflammatory cytokines activates receptor-associated JAKs,

leading to the phosphorylation of STATs [7]. Activated cytoplasmic STATs form homo- or hetero-dimers, translocate to the nucleus, and function as transcription factors to regulate the expression of target genes such as inflammatory mediators [8]. As the JAK-STAT signaling pathway is also involved in the mediation of inflammation-related gene expression, it is important to strictly regulate or inhibit its activation to prevent inflammation and treat diseases.

Allium cepa L. (*A. cepa*) is a perennial plant belonging to the Liliaceae family and one of the oldest cultivated plants worldwide. It has been used for food and medicinal purposes as an antipyretic, anthelmintic, stroke remedy, and for lowering blood cholesterol in the world [9]. Blood cholesterol-lowering, antioxidant, anti-cancer, and anti-inflammatory effects have also been investigated [10-12]. These onions contain more flavonoids in the peel than in the edible parts; in particular, the content of quercetin, which has excellent anticancer and anti-inflammatory effects and is the main flavonoid component of onions, is also higher in the peel [13, 14]. However, the peel of *A. cepa* is typically used as feed or discarded, despite its potential physiological functionality. By exploring the health benefits of onion peel, which is currently not used as an edible part of food, it is possible to reduce waste and promote economic feasibility while protecting the environment [15]. Therefore, investigating the anti-inflammatory effects of onion peel is a valuable research direction with implications for environmental protection

and utilizing waste resources. *A. cepa* peel extract reportedly has anti-oxidant, detoxification and anti-inflammatory effects by suppressing LPS-induced inflammatory mediators in HT-29 human colon carcinoma cells and RAW264.7 mouse macrophage cells [16, 17]. However, the efficacy comparison according to the extraction method and the detailed mechanism as an anti-inflammatory ingredient remains to be explored.

The purpose of this study is to compare the anti-inflammatory effects of *A. cepa* peel extracts obtained using various extraction methods and investigate detailed mechanism underlying of them. To assess the anti-inflammatory efficacy of *A. cepa* peel extracts obtained using various extraction methods, I prepared extracts using hot water, 30% ethanol, and 50% ethanol, and examined their effects. These results indicated that the AP50E extract had the most potent anti-inflammatory effect in LPS-induced RAW264.7 mouse macrophages by directly inhibiting JAK-STAT signaling.

MATERIAL AND MATHODS

1. Antibodies used in this study.

Anti-iNOS (sc-651), anti-IκBα (sc-371) and anti-p38 (sc-535) were purchased from Santa Cruz Biotechnology (Santa Cruz, CA, USA). Anti-pS-IκBα (#2859), anti-pS-NF-κB (#3033), anti-NF-κB (#8242), anti-pT/Y-p44/42 MAPK (Erk1/2) (#9101), anti-p44/42 MAPK (Erk1/2) (#4695), anti-pT/Y-SAPK/JNK (#9251), anti-SAPK/JNK (#9252), anti-pT/Y-p38 (#4631), anti-pY-STAT1 (#8826), anti-STAT1 (#8826), anti-pY-STAT3 (#9145), anti-STAT3 (#30835), anti-pY-STAT5 (#9359), anti-STAT5 (#9363), anti-pY-JAK1 (#3331), anti-JAK1 (#3332), pY-JAK2 (#3776) and anti-JAK2 (#3230) were purchased from Cell Signaling Technology (Danvers, MA, USA), while and anti-α-Tubulin (A01080) was from Abbkine (Wuhan, China). The horseradish peroxidase (HRP)-tagged anti-rabbit antibody (ADI-SAB-300) and HPR-tagged anti-mouse antibody (ADI-SAB-100) was purchased from Enzo Life Sciences (Farmingdale, NY, USA). The antibody information is summarized in Supplementary Table 1.

2. Reagents used in this study.

2,2'-Azin-obis-(3-ethylbenzothiazoline-6-sulfonic acid) (ABTS, A1888), potassium persulfate (P5592), Quercetin (Q4951), Lipopolysaccharide (LPS, L3012) and Griess reagent (G4410) were purchased from Sigma Aldrich (St.

Louis, MO, USA). Diethylene glycol was purchased from JUNSEI CHEMICAL Co. LTD (Tokyo, Japan). NaOH (1310-73-2) was obtained from DAEJUNG CEHEMICALS & METALS (Seoul, Republic of Korea). 3-(4,5-dimethylthiazol-2-Yl)-2,5-diphenyltetrazolium bromide (MTT) reagent (M1415) was purchased from Duchefa Biochemie (Haarlem, Netherlands). The reagent information is summarized in Supplementary Table 2.

3. *A. cepa* peel preparation and extraction

The plant name of *Allium cepa* L. (*A. cepa*) has been checked with http://www.theplantlist.org on April 09 and the outer peel of *A. cepa* used in this study was collected from Muan-gun, Jeollanam-do, Korea. *A. cepa* peel hot water extract (APW) was extracted with 20 volumes of hot water twice for 8 h at 90 °C, *A. cepa* peel 30% EtOH extract (AP30E) were extracted with 20 volumes (w/v) 30% ethanol twice for 8 h at 60 °C and *A. cepa* peel 50% EtOH extract (AP50E) were extracted with 20 volumes 50% ethanol twice for 8 h at 40 °C. The extract was passed through a 25 μm filter (Whatman, Tokyo, Japan) and concentrated by the concentrate tank at 65 °C, at 600 – 700 mH reduced pressure and lyophilized using a freeze dryer. The extraction process is illustrated in Fig. 1A.

4. Estimation of total flavonoids contents

After mixing *A. cepa* peel extracts, diethylene glycol and sodium hydroxide in a 1:10:10 ratio, react for 1 h at 37 °C. Absorbance was measured at 420 nm using a microplate reader (Tecan, Männedorf, Switzerland). The standard curve for calibration was constructed using quercetin following the procedure described earlier. The total flavonoid content of each extract is expressed as milligrams of quercetin equivalents per gram of sample (mg QE/g).

5. ABTS radical scavenging activity assay

After mixing a 7.4 mM ABTS and 2.6 mM potassium persulfate in a 1:1 ratio and allowed to react for 12 h at room temperature in the dark. The ABTS solution was diluted with 99% ethanol. The diluted ABTS solution and *A. cepa* peel extract were mixed in a 1:1 ratio and allowed to react for 7 min at room temperature in the dark. The absorbance was measured at 570 nm using a microplate reader (Tecan).

6. HPLC fingerprint analysis

Each 200 mg of *A. cepa* peel extracts were dissolved in 10 mL of 80% methanol solvent, ultrasonic extraction for 1 h, shaking for 1 h, and filtering with a 0.2 μm filter (Sartorius, Goettingen, Germany). Chemical fingerprint analysis of *A. cepa* peel extracts was carried out using an Ultimate3000 HPLC (Thermo Fisher Scientific, Waltham, MA, USA). Detailed HPLC

conditions are described in Supplementary Table 3.

7. Cell line and culture

The mouse macrophage cell line RAW264.7 used in this study was obtained from the American Type Culture Collection (ATCC). The cells were cultured in Dulbecco's Modified Eagle's medium (DMEM, HyClone, Logan, UT, USA) containing 10% heat-inactivated fetal bovine serum (FBS, HyClone) and 1% penicillin/streptomycin (Capricorn Scientific GmbH, Ebsdorfergrund, Germany). The cells were incubated at a humidified incubator (Vision Science, Seoul, Korea) in 5% CO2 at 37 °C.

8. Cell viability assay

RAW264.7 cells were seeded and treated with different concentrations of *A. cepa* extract for 24 h. After treatment, cells were treated with MTT and incubated for 2 h. The formazan crystals were dissolved in DMSO and the absorbance was determined at 570 nm using a plate reader (Tecan).

9. Nitric oxide (NO) assay

RAW264.7 cells were seeded then pre-treated with various concentrations of *A. cepa* peel extracts for 2 h and LPS was added for 16 h. To determine NO production, 100 μL of the conditioned culture medium was added to an equal volume of Griess reagent for 10 min in the dark. The absorbance was measured at 540 nm using a plate reader (Tecan).

10. Western blot

After treatment, cells were washed twice with cold PBS and lysed in 1% Triton X-100 buffer containing phosphatase and protease inhibitors. After incubating the lysate on ice for 10 min, debris was removed by centrifugation at 13,200 rpm for 10 min at 4 °C; the supernatant was then collected. Equal amounts of protein were loaded into each well, separated by SDS-polyacrylamide gel electrophoresis (SDS-PAGE), and transferred onto nitrocellulose (NC) membranes. The membranes were blocked in 5%-skimmed milk and subsequently incubated with specific primary antibodies against the target proteins diluted to 1:1,000 in Tris-buffered saline with 0.1% Tween 20 (TBS-T) at 4°C overnight. The next day, membranes were incubated with HRP-conjugated secondary antibodies at room temperature for 1 h. Signals were visualized using ECL chemiluminescence substrate (DYNE BIO, Seongnam, Korea).

11. RNA isolation, reverse transcription, and quantitative real-time PCR

After treatment, total RNA was extracted using TRIzol reagent (Takara, Shiga, Japan), and reverse transcription and cDNA synthesis were performed using the ReverTra Ace qPCR RT Master Mix kit (TOYOBO, Osaka, Japan). Quantitative real-time PCR was performed using SYBR Green qPCR Master Mix (Applied Biological Materials, Richmond,

Canada). The results were calculated using the GAPDH expression levels. Primer sequences are listed in Supplementary Table 4.

12. Enzyme-linked immunosorbent assay (ELISA)

RAW264.7 cells were pre-treated with various concentrations of AP50E for 2 h and LPS was added for 16 h. Culture media were collected, and cytokines levels were measured by IL-1β (MLB00C), IL-6 (M6000B), and TNF-α (MTA00B) ELISA kit (R&D Systems, Minneapolis, MN, USA).

13. Cytokine array

RAW264.7 cells were pretreated with AP50E for 2 h, and LPS was added for 16 h. Culture supernatants were collected and cytokines were measured using the Mouse Cytokine Array Panel kit (ARY006, R&D Systems).

14. Conditioned medium from LPS-mediated macrophages (LPS-CM) and heat-inactivated CM.

After activating RAW264.7 cells for 4 h with LPS treatment, remove the media, washed with PBS, changed it with a new medium, and incubated for another 4 h. Heat-inactivated CM was prepared by heating LPS-CM at 100 °C for 20 min and used as a negative control.

15. Dataset analysis

The microarray dataset used in this study was GSE160086 [18]. The Z-scores for each gene of interest were calculated and displayed using a heap map.

16. Statistical analysis

All results are expressed as means ± standard deviation (SD) of three independent experiments. Statistical significance was determined by unpaired Student's *t*-test, and differences were considered significant when a p-value < 0.05.

RESULTS

1. Total amount of flavonoids, antioxidant activity and HPLC analysis of the various *A. cepa* peel extracts

To investigate the anti-inflammatory effects of *A. cepa* peel extracts, three samples were extracted using hot water, 30% EtOH, and 50% EtOH (Figure 1). Because flavonoids are known to have anti-inflammatory properties [19], I determined the total flavonoid content in each *A. cepa* peel extract and found that the total flavonoid content was higher in *A. cepa* peel EtOH extracts than in APW (Figure 2). In particular, among the flavonoids, kaempferol and quercetin are flavonoids with excellent anti-inflammatory properties [20, 21]. From the results of the HPLC finger analysis, kaempferol and quercetin contents were higher in *A. cepa* peel EtOH extracts than in APW (Figure 3 and Table 5-7). Oxidative stress plays an important role in the occurrence and progression of inflammation and leads to inflammation-related diseases [22]. Therefore, the mitigation of oxidative stress by antioxidants is important for suppressing inflammation [23, 24]. Accordingly, the antioxidant activity of *A. cepa* peel extracts was evaluated using the ABTS assay, and the antioxidant activity was also higher in *A. cepa* peel EtOH extracts than in APW (Figure 4). Based on these results, I expected that the *A. cepa* peel EtOH extracts would have a greater anti-inflammatory effect than the APW.

2. AP50E significantly suppresses LPS-induced inflammation among the *A. cepa* peel extracts in RAW 264.7 cells

To confirm the anti-inflammatory effects of *A. cepa* peel extract, I used a model in which inflammation was induced by treating LPS to RAW264.7 cells. Prior to the experiment, the cytotoxicity of each extract according to the extraction methods of *A. cepa* peel was confirmed in a concentration-dependent manner using the MTT assay. In cell viability assay, APW and AP30E exhibited no significant cytotoxicity up to 160 μg/mL, while AP50E was cytotoxic at 160 μg/mL (Figure 5A-C). Since all extracts showed no cytotoxicity up to 80 μg/mL, I confirmed the anti-inflammatory effects of each *A. cepa* peel extracts at 80 μg/mL. LPS induces inflammation and alters macrophage morphology [25]. Therefore, I investigated whether *A. cepa* peel extract could prevent LPS-induced morphological changes in RAW264.7 cells. APW did not; however, AP30E and AP50E considerably inhibited morphological activation (Figure 6). When I further confirmed the anti-inflammatory efficacy of *A. cepa* peel extracts, LPS-induced NO production and iNOS mRNA and protein expression were most significantly reduced by AP50E compared to the other extracts. (Figure 7-8). Based on these results, I found that AP50E had the highest anti-inflammatory potency among all *A. cepa* peel extracts.

3. AP50E inhibits IL-1β and IL-6 production and JAK-STAT activation in LPS-induced RAW264.7 cells

Since AP50E best inhibited LPS-induced inflammation, I investigated which LPS-induced downstream signals of inflammation were inhibited by AP50E. Since NFκB/IκBα and MAPK signaling are representative inflammation-related signals, I hypothesized that AP50E could prevent LPS-induced NFκB/IκBα and MAPK activation. Surprisingly, AP50E could not prevent LPS-induced activation of NFκB/IκBα and MAPK signaling (Figure 9A, B and 10A, B). I also confirmed JAK-STAT signaling because JAK-STAT signaling is also associated with LPS-induced inflammation signals, and confirmed that the activation of JAK1, 2 and STAT1, 3 and 5 was significantly prevented by AP50E (Figure 9C, D and 10C, D). When activated by exposure to external stimuli, macrophages phagocytose these pathogens and secrete pro-inflammatory cytokines to activate and recruit other inflammatory cells to the site of inflammation [26]. Inflammatory cytokines such as IL-1, IL-6, TNFα are mainly produced by activated macrophages [27]. To further investigate the anti-inflammatory effects of AP50E, changes in the expression of representative pro-inflammatory cytokines by AP50E were investigated. The LPS-induced mRNA expressions of IL-1β and IL-6 considerably decreased by AP50E but that of TNF-α mRNA did not (Figure 11A-C). In addition, IL-1β and IL-6 productions had considerably decreased but that of TNF-α did not (Figure

11D-F). Therefore, I suggested that AP50E inhibits the activation of LPS-induced JAK-STAT pathway and production of pro-inflammatory cytokines IL-1b and IL-6.

4. AP50E inhibits inflammatory IL-1α and IL-27 in LPS-induced RAW264.7 cells

Apart from the previously identified representative LPS-induced pro-inflammatory cytokines such as IL-1β, IL-6, and TNF-α, there are many others that can cause inflammation [26]. And pro-inflammatory cytokines are important therapeutic targets for suppressing inflammation [28]. Therefore, I hypothesized that AP50E exhibits anti-inflammatory effects through inhibition of other pro-inflammatory cytokines besides IL-1β and IL-6. First, using the GSE160086 database, I analyzed representative cytokines and found the upregulated 23 genes in LPS-induced RAW264.7 groups (Figure 12A). Next using the cytokine array, IL-1α and IL-27 were identified as cytokines that were LPS-induced and prevented by AP50E (Figure 12B-D). IL-27 binding to IL-27 receptor is associated with pro-inflammatory responses and activates JAK-STAT signaling in macrophages [29], and IL-1α secreted from activated macrophages is also known as a pro-inflammatory cytokine, and unregulated expression causes acute or chronic inflammation such as fever and sepsis [30]. Through mRNA expression analysis, it was confirmed that the expression of IL-1α and IL-27 induced by

LPS were reduced by AP50E (Figure 12E, F). These findings suggest that AP50E not only significantly prevented pro-inflammatory cytokines such as IL-1β and IL-6, but also IL-1α and IL-27.

5. AP50E blocks the JAK-STAT axis in a direct manner

Previously, I verified that AP50E inhibits the activation of JAK-STAT by suppressing the expression of pro-inflammatory cytokines such as interleukins. However, I wondered whether AP50E could directly prevent the activation of JAK-STAT independently of the reduction in pro-inflammatory cytokines. To rule out differences in the amount of inflammatory molecules reduced by AP50E, I collected conditioned medium from LPS-stimulated RAW264.7 cells (LPS-CM) containing equal amounts of pro-inflammatory cytokines and treated with it to RAW264.7 cells (Figure 13). LPS treatment induced JAK-STAT activation at 4 h (Figure 9C, D), but LPS-CM treatment, which collected pro-inflammatory cytokines, induced JAK-STAT activation at 30 min (Figure 14). In addition, because pro-inflammatory mediators are denatured by heat, LPS-CM inactivated by heat shock was used as a negative control. When the cells were treated with LPS-CM, JAK-STAT was rapidly activated within 30 min, but this was prevented by AP50E (Figure 15). These results suggest that AP50E directly inhibits JAK-STAT independently of cytokine reduction. In conclusion, our results suggested that AP50E prevents activation of JAK-STAT both in a

direct manner and in a manner that reduces expression of pro-inflammatory cytokines such as IL-1α, IL-1β, IL-6 and IL-27 (Figure 16).

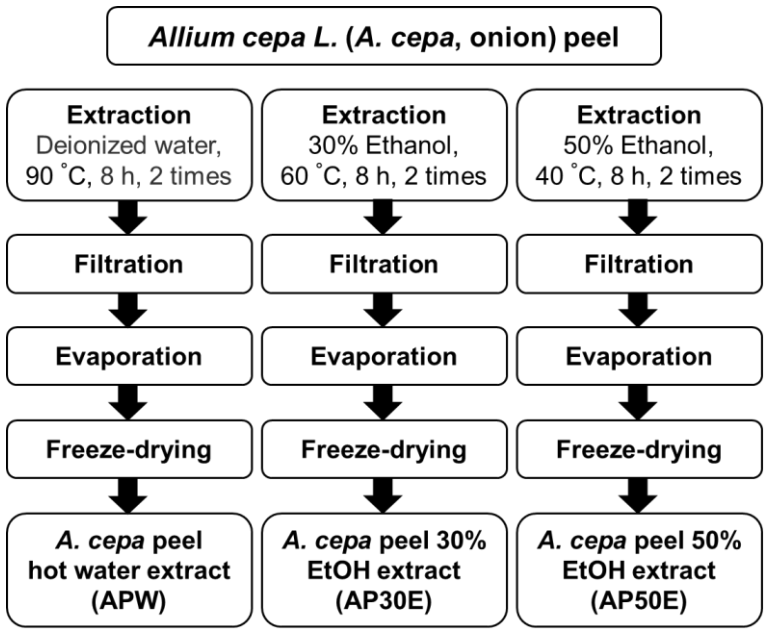

Figure 1. Overview of the extraction method of *A. cepa* peel extracts

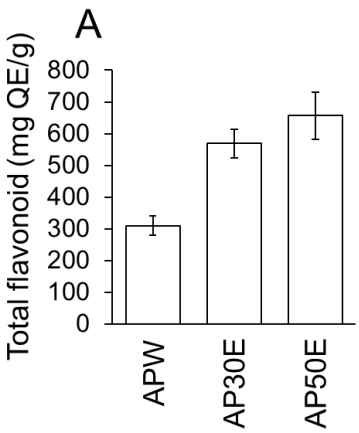

B

Sample	Total flavonoid (mg/g QE)
A. cepa peel hot water extract (APW)	309.79 (±29.88)
A. cepa peel 30% EtOH extract (AP30E)	568.75 (±45.68)
A. cepa peel 50% EtOH extract (AP50E)	656.46 (±74.07)

Figure 2. Total amount of flavonoids of the various *A. cepa* peel extracts

(A, B) After mixing *A. cepa* peel extracts, diethylene glycol and sodium hydroxide in a 1:10:10 ratio, react for 1 h at 37 ℃. Absorbance was measured at 420 nm using a microplate reader.

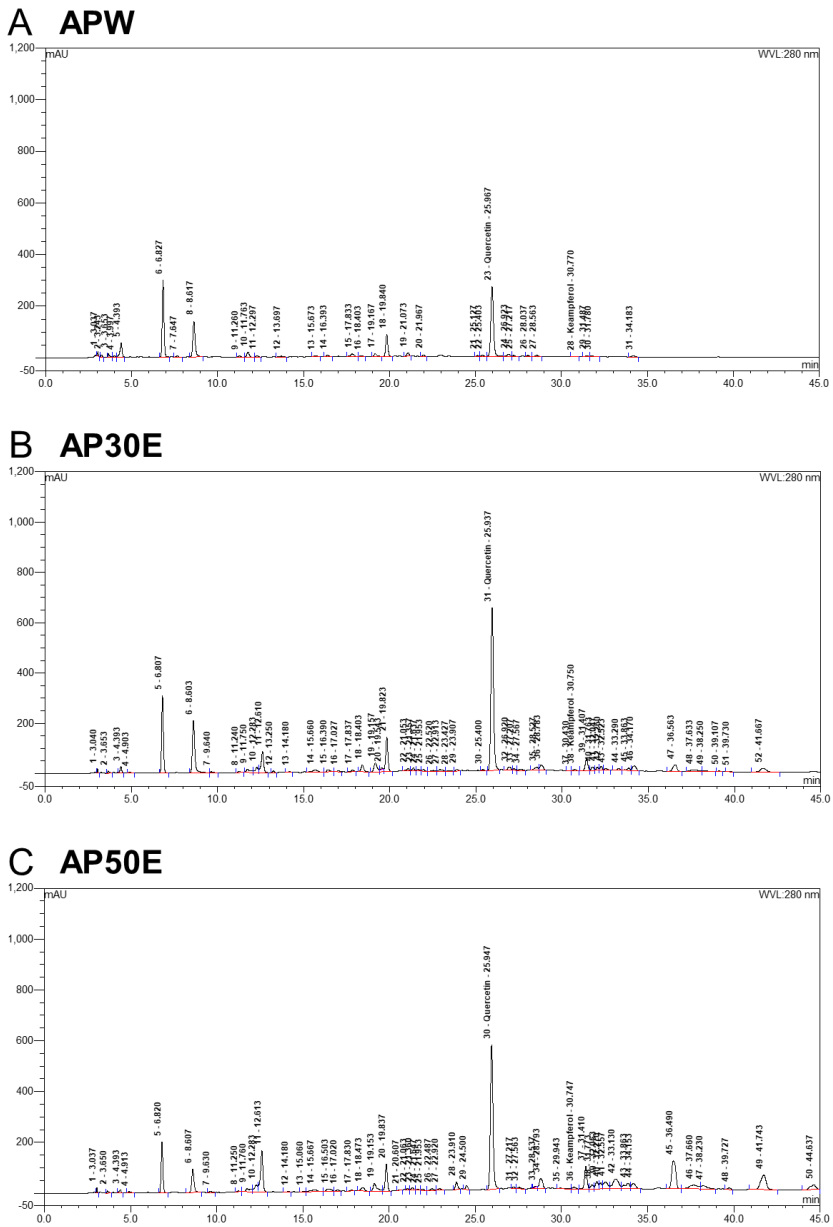

Figure 3. HPLC analysis of the various *A. cepa* peel extracts

(A-C) Representative HPLC chromatograms of APW(A), AP30E(B) and AP50E(C).

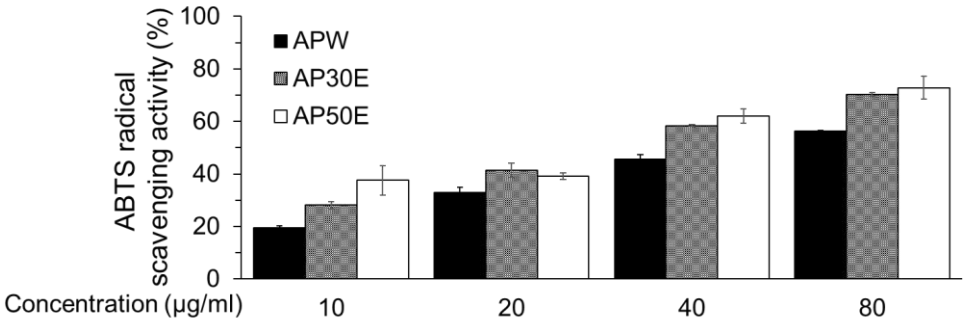

Figure 4. Antioxidant activity of the various *A. cepa* peel extracts

Antioxidant activity of the various *A. cepa* peel extracts was determined using ABTS radical scavenging activity assay.

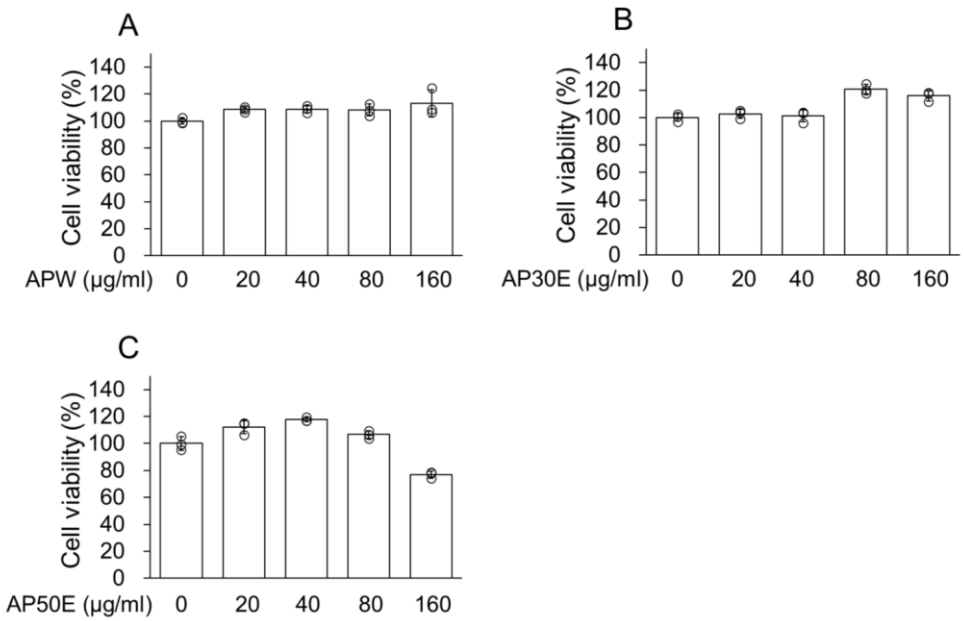

Figure 5. Cell viability of *A. cepa* peel extracts according to extraction method

(A-C) RAW264.7 cells were treated with various *A. cepa* extracts at the indicated concentrations for 24 h. Cell viability was evaluated using the MTT assay.

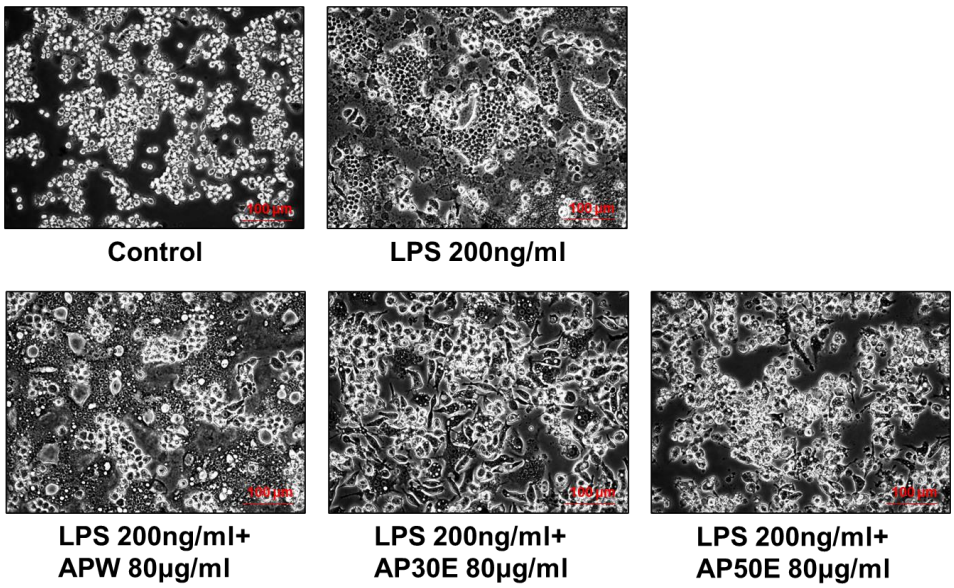

Figure 6. AP30E and AP50E considerably inhibited morphological activation

Raw264.7 cells were pre-treated with various *A. cepa* peel extracts for 2 h and LPS was added for 16 h. Morphological alteration of RAW264.7 cells are observed. Scale bar: 100 μm

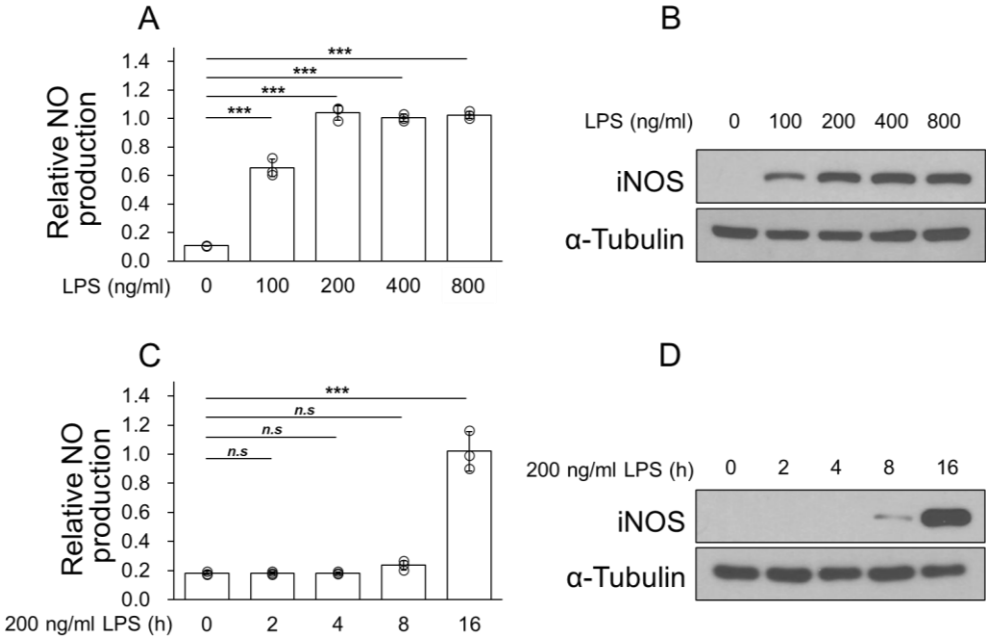

Figure 7. Level of NO production and iNOS expression according to LPS-treated concentration and time in RAW264.7 cells

(A, B) RAW264.7 cells were treated with LPS at the indicated concentrations for 16 h. NO levels were determined using Griess reagent (A). Relative protein expression was analyzed by western blotting (B).

(C, D) RAW264.7 cells were treated with LPS (200 ng/ml) for indicated times. NO levels were determined using Griess reagent (C). Relative protein expression was analyzed by western blotting (D).

Statistical significance was determined using an unpaired Student's *t*-test. ***$p < 0.001$.

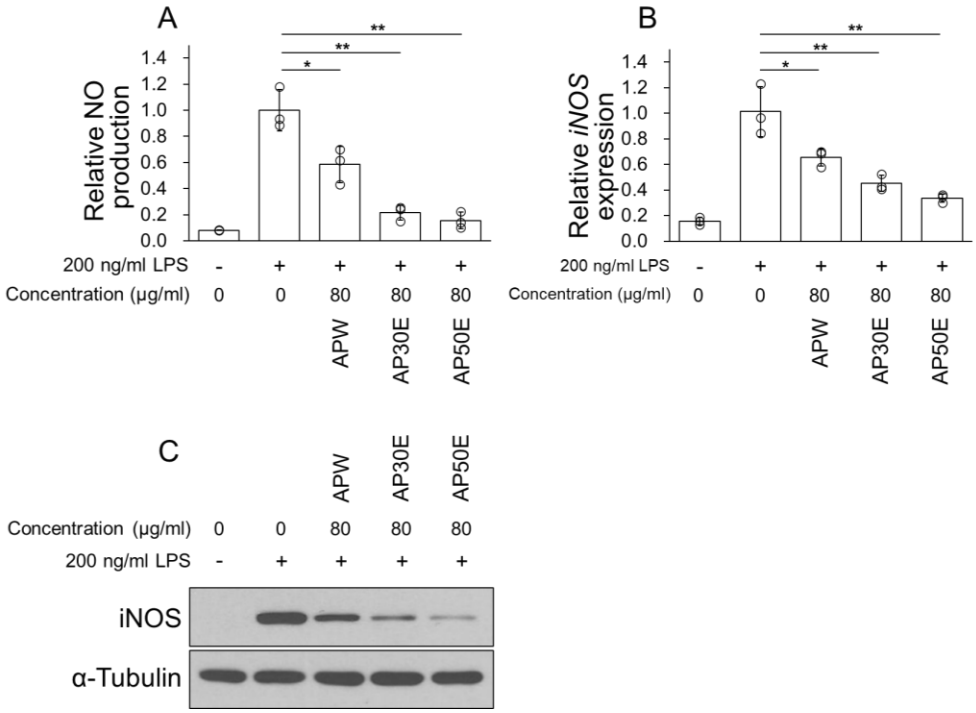

Figure 8. AP50E significantly suppresses LPS-induced NO production and iNOS expression among various *A. cepa* peel extracts in RAW264.7 cells

(A-C) Raw264.7 cells were pre-treated with various *A. cepa* peel extracts for 2 h and LPS was added for 16 h. NO levels were determined using Griess reagent (A). Relative mRNA expression was analyzed by RT-qPCR (B). Relative protein expression was analyzed by western blotting (C). Statistical significance was determined using an unpaired Student's *t*-test. * $p < 0.05$ and ** $p < 0.01$

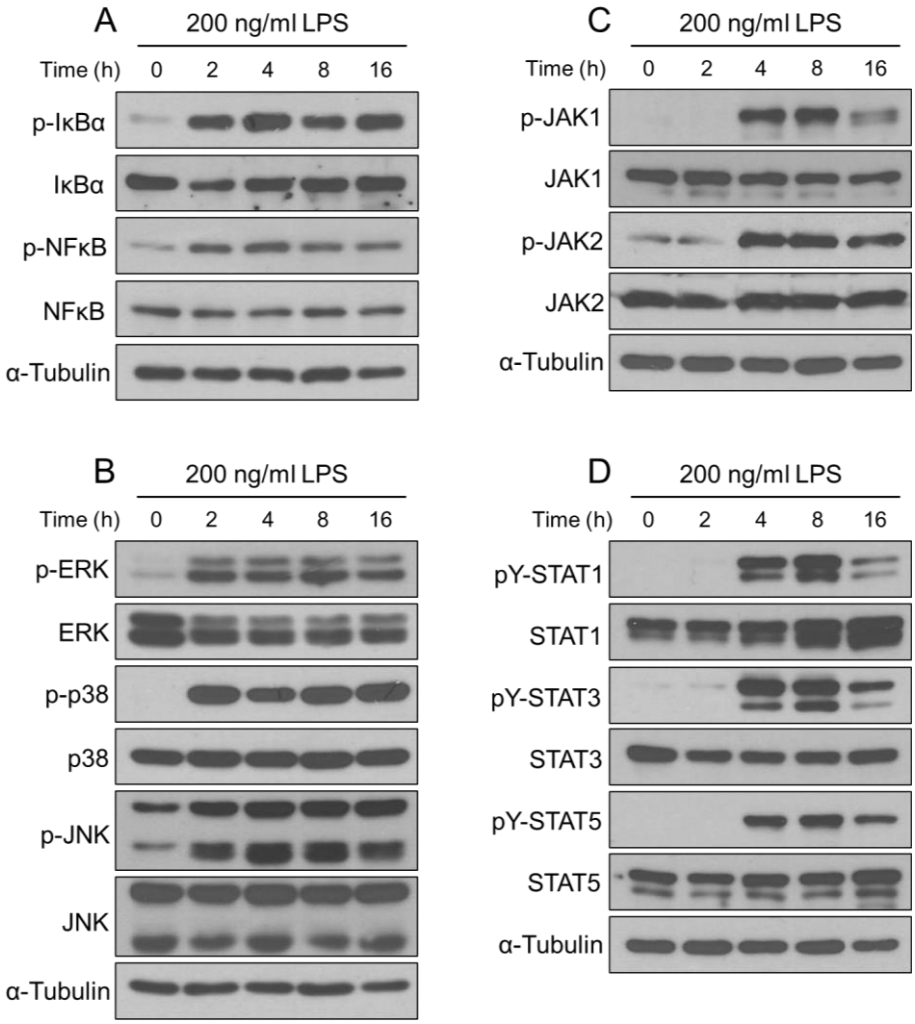

Figure 9. Activation of IκBα/NF-κB, MAPK and JAK-STAT signaling according to LPS-treated time in RAW264.7 cells

(A-D) RAW264.7 cells were treated with 200 ng/ml LPS for indicated times. Relative protein expression was analyzed by western blotting.

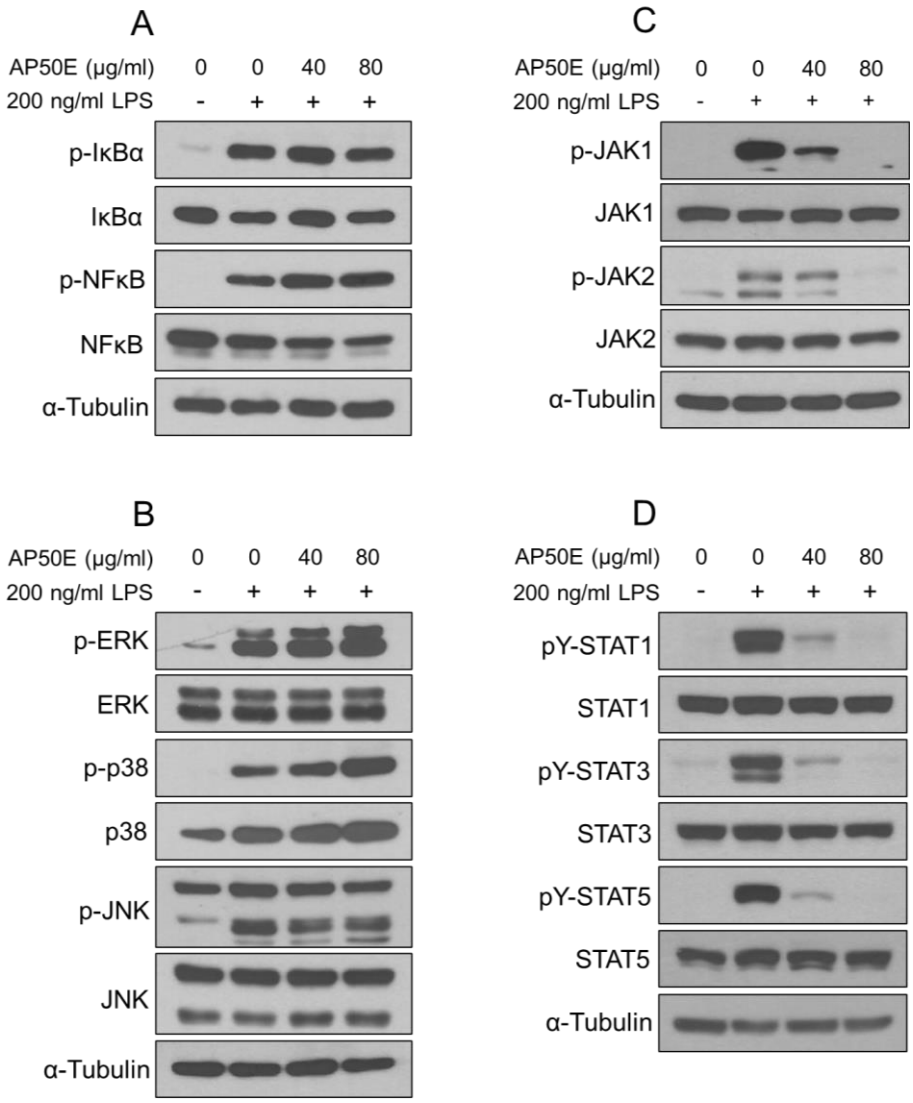

Figure 10. AP50E inhibits JAK-STAT activation in LPS-induced RAW264.7 cells

(A-D) RAW264.7 cells were pre-treated with AP50E extract for 2 h and LPS was added for 4 h. The relative protein expression was analyzed by western blotting.

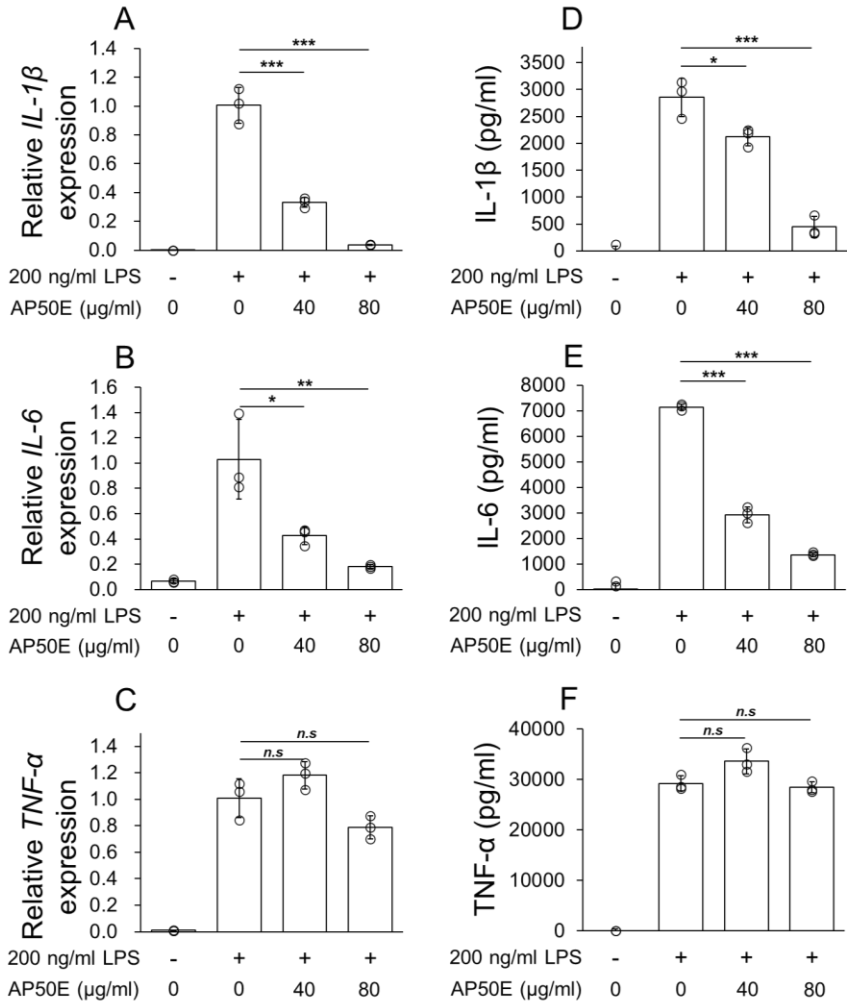

Figure 11. AP50E inhibits IL-1β and IL-6 production in LPS-induced RAW264.7 cells

(A-F) RAW264.7 cells were seeded in 6-well plate then pre-treated with AP50E for 2 h and LPS was added for 16 h. The relative mRNA expression was analyzed by RT-qPCR (A-C). Produced cytokines are measured by ELISA. (D-F)

Statistical significance was determined using an unpaired Student's *t*-test. * $p < 0.05$, ** $p < 0.01$, and *** $p < 0.001$.

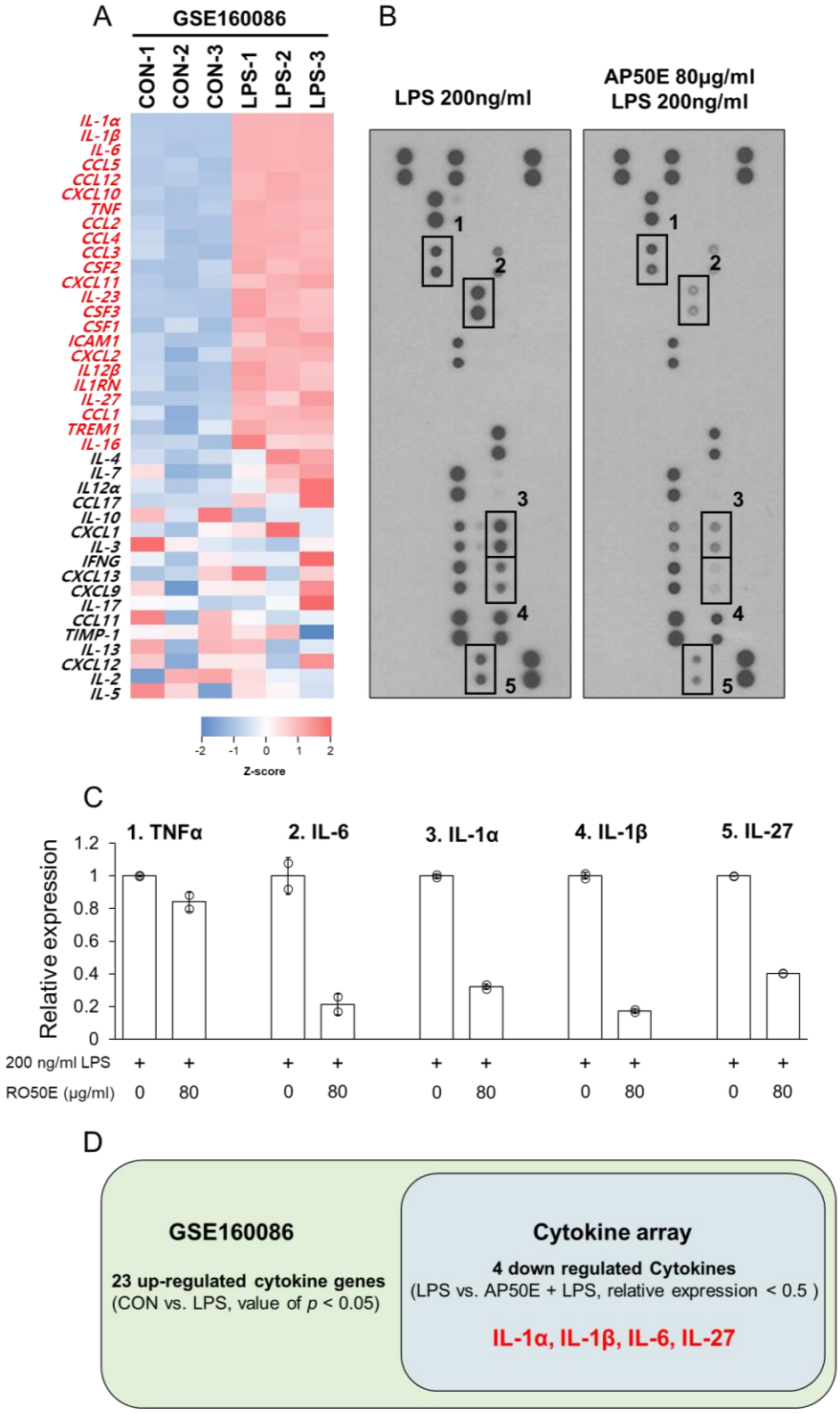
A
GSE160086
CON-1
CON-2
CON-3
LPS-1
LPS-2
LPS-3
IL-1α
IL-1β
IL-6
CCL5
CCL12
CXCL10
TNF
CCL2
CCL4
CCL3
CSF2
CXCL11
IL-23
CSF3
CSF1
ICAM1
CXCL2
IL12β
IL1RN
IL-27
CCL1
TREM1
IL-16
IL-4
IL-7
IL12α
CCL17
IL-10
CXCL1
IL-3
IFNG
CXCL13
CXCL9
IL-17
CCL11
TIMP-1
IL-13
CXCL12
IL-2
IL-5
-2
-1
0
1
2
Z-score
B
LPS 200ng/ml
AP50E 80μg/ml
LPS 200ng/ml
1
2
3
4
5
C
1. TNFα
2. IL-6
3. IL-1α
4. IL-1β
5. IL-27
Relative expression
1.2
1
0.8
0.6
0.4
0.2
0
200 ng/ml LPS
RO50E (μg/ml)
0
80
D
GSE160086
23 up-regulated cytokine genes
(CON vs. LPS, value of p < 0.05)
Cytokine array
4 down regulated Cytokines
(LPS vs. AP50E + LPS, relative expression < 0.5)
IL-1α, IL-1β, IL-6, IL-27

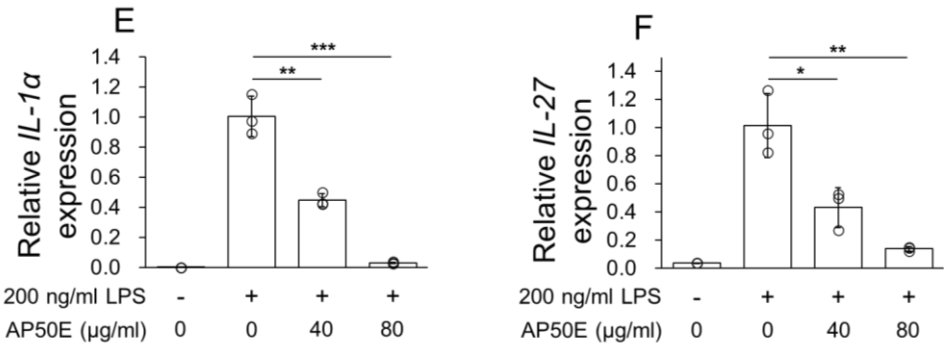

Figure 12. AP50E inhibits inflammatory IL-1α and IL-27 in LPS-induced RAW264.7 cells

(A) Heatmap of each mRNA expression of each gene between LPS treated and control (CON) group of RAW264.7 cells, based on the GSE160086 dataset. Blue represents low expression and red represents high expression.

(B, C) RAW264.7 cells were pre-treated with AP50E for 2 h and LPS was added for 16 h. Produced cytokines were measured using a cytokine array (B) and cytokine blots were analyzed using ImageJ (C).

(D) Illustration showing upregulated 23 genes in LPS-treated RAW264.7 groups in GSE160086, and among them, downregulated 4 cytokines in the AP50E+LPS treatment group compared to the LPS treatment group in the cytokine array.

(E-F) RAW264.7 cells were pretreated with AP50E for 2 h, and LPS was added for 16 h. Relative mRNA expression was analyzed by RT-qPCR. Statistical significance was determined using an unpaired Student's *t*-test. *$p < 0.05$, **$p < 0.01$, and ***$p < 0.001$.

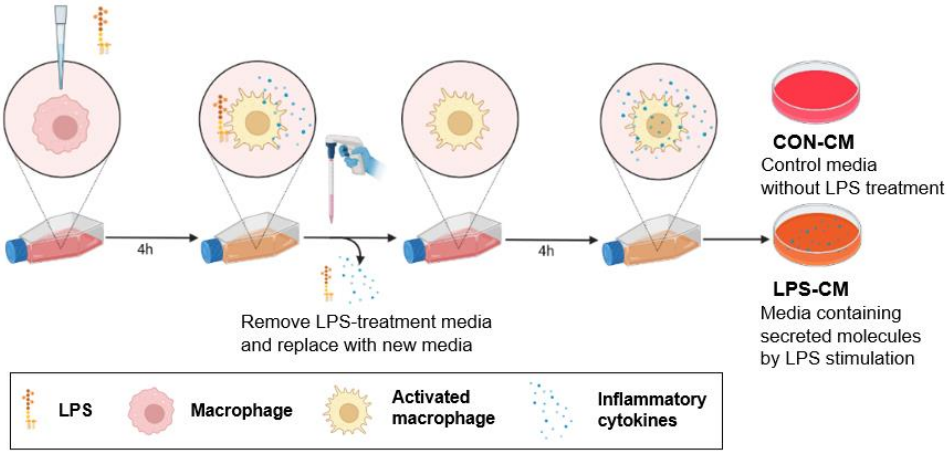

Figure 13. Schematic figure of CON-CM and LPS-CM collection.

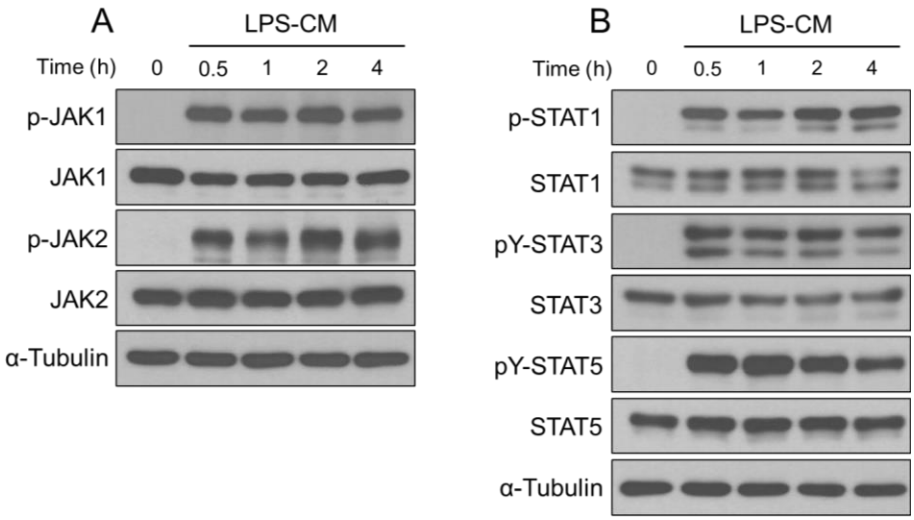

Figure 14. Activation of JAK-STAT signaling according to LPS-CM treated time in RAW264.7 cells

(A, B) RAW264.7 cells were treated with LPS-CM for indicated times. Relative protein expression was analyzed by western blotting.

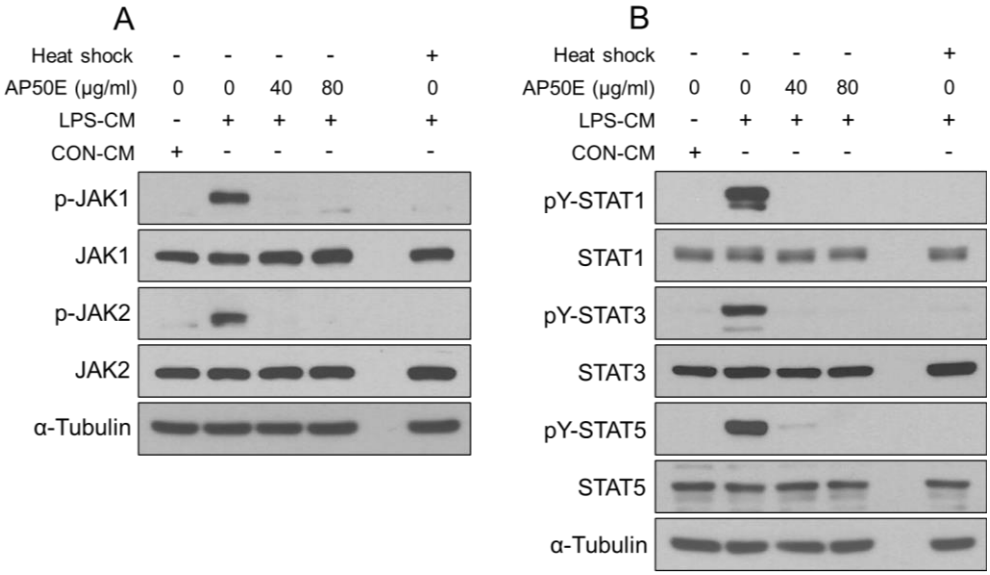

Figure 15. AP50E blocking the JAK-STAT axis in a direct manner

(A, B) RAW264.7 cells were pretreated with the AP50E extract for 2 h and exchanged with CON-CM or LPS-CM with AP50E for 30 min. Relative protein expression was analyzed by western blotting. The schematic figure was created using BioRender.com.

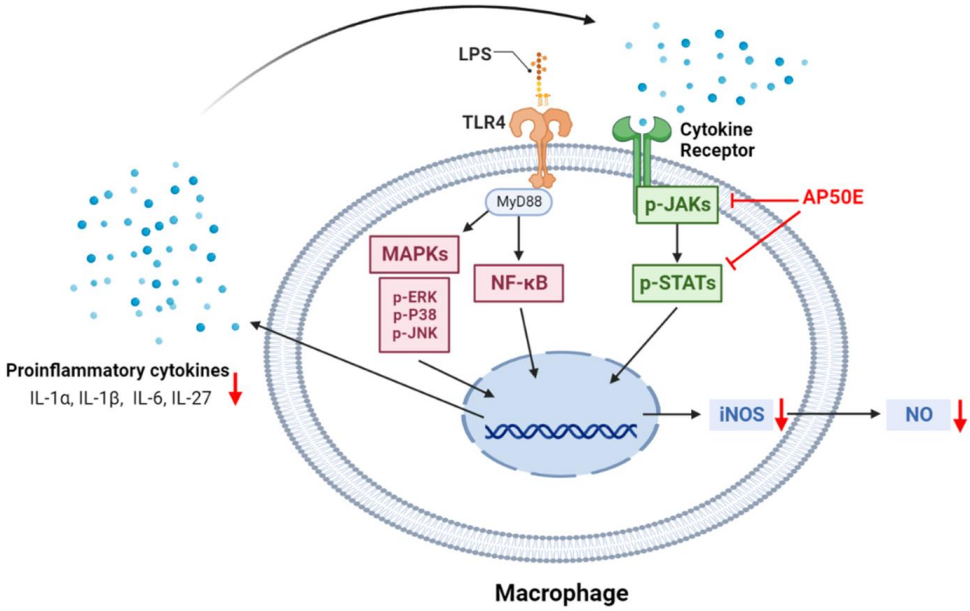

Figure 16. Graphical summary of this study

AP50E most effectively prevented the production of iNOS, an enzyme related to inflammation and inflammatory mediators such as NO, IL-1α, IL-1β, IL-6 and IL-27. AP50E directly inhibits the JAK-STAT axis, which is associated with inflammation.

Table 1. Antibodies used in this study

Antibody	Cat. No.	Company
α-Tubulin	A01080	Abbkine (Wuhan, China)
iNOS (NOS2)	sc-651	Santa Cruz Biotechnology (Santa Cruz, CA, USA)
IκBα	sc-371	
p38	sc-535	
pS-IκBα	#2859	Cell Signaling Technology (Danvers, MA, USA)
pS-NFκB	#3033	
NFκB	#8242	
pT/Y-p44/42 MAPK (Erk1/2)	#9101	
p44/42 MAPK (Erk1/2)	#4695	
pT/Y-SAPK/JNK	#9251	
SAPK/JNK	#9252	
pT/Y-p38	#4631	
pY-STAT1	#8826	
STAT1	#9172	
pY-STAT3	#9145	
STAT3	#30835	
pY-STAT5	#9359	
STAT5	#9363	
pY-JAK1	#3331	
JAK1	#3332	
pY-JAK2	#3776	
JAK2	#3230	
HRP-tagged anti-rabbit	ADI-SAB-300	Enzo Life Science (Farmingdale, NY, USA)
HRP-tagged anti-mouse	ADI-SAB-100	

Table 2. Reagents used in this study

Reagents	Cat. No.	Company
Diethylene glycol	111-46-6	JUNSEI CHEMICAL CO., LTD (Tokyo, Japan)
Sodium hydroxide	1310-73-2	DAEJUNG CHEMICALS & METALS (Seoul, Republic of Korea)
2,2'-azin-obis-(3-ethylbenzothiazoline-6-sulfonic acid) (ABTS)	A1888	Sigma Aldrich (St. Louis, MO, USA)
Potassium persulfate	P5592	
Quercetin	Q4951	
Lipopolysaccharide (LPS)	L3012	
Griess reagent	G4410	
MTT	M1415	Duchefa Biochemie (Haarlem, Netherlands)
IL-1β ELISA Kit	MLB00C	R&D System (Minneapolis, MN, USA)
IL-6 ELISA Kit	M6000B	
TNF-α ELISA Kit	MTA00B	
Mouse Cytokine Array Kit	ARY006	

Table 3. Summary of HPLC analysis conditions

Instrument	Ultimate 3000 HPLC (Thermo Dionex, USA)		
Column	INNO C18 column (YoungjinBiochrom, Korea 4.6 x 250,5 um)		
Injection volume	10 μl		
Flow rate	1 ml/min		
Scanning	190–400 nm DAD scanning		
Detection wavelength	280 nm		
Temperature	40 ℃		
Software	Chromeleon 6.8		
Mobile Phase	**Time (min)**	**0.1% TFA in DW (%)**	**Acetonitrile (%)**
	0	90	10
	1	90	10
	40	50	50
	50	0	100
	55	0	100
	56	90	10
	60	90	10

Table 4. Primer sequences used in this study

Gene name	Direction	Sequence (5′–3′)
iNOS (mouse)	Forward	CAGCACAGGAAATGTTTCAGC
	Reverse	TAGCCAGCGTACCGGATGA
IL-1β (mouse)	Forward	TTGACGGACCCCAAAAGATG
	Reverse	AGAAGGTGCTCATGTCCTCA
IL-6 (mouse)	Forward	GGTGACAACCACGGCCTTCCC
	Reverse	AAGCCTCCGACTTGTGAAGTGGT
TNF-α (mouse)	Forward	TATGGCTCAGGGTCCAACTC
	Reverse	CTCCCTTTGCAGAACTCAGG
IL-1α (mouse)	Forward	ACGGCTGAGTTTCAGTGAGACC
	Reverse	CACTCTGGTAGGTGTAAGGTGC
IL-27 (mouse)	Forward	CACCTCCGCTTTCAGGTGC
	Reverse	AGGTATAGAGCAGCTGGGGC
GAPDH (mouse)	Forward	GCAAATTCAACGGCACAG
	Reverse	CACCAGTAGACTCCACGAC

Table 5. HPLC fingerprint Peak table of APW

Peak No.	Ret. Time (min)	Height (mAU)	Area (mAU*min)	Name	Amount (mg/kg)
1	3.04	18.226	1.043		
2	3.24	7.000	0.638		
3	3.65	14.802	1.649		
4	4.00	6.161	0.675		
5	4.39	54.835	7.657		
6	6.83	298.156	35.623		
7	7.65	4.188	0.635		
8	8.62	138.017	21.986		
9	11.26	4.935	0.789		
10	11.76	19.686	3.141		
11	12.30	5.677	0.706		
12	13.70	3.292	0.836		
13	15.67	3.535	0.771		
14	16.39	5.826	0.913		
15	17.83	10.246	2.558		
16	18.40	3.196	0.696		
17	19.17	10.103	2.037		
18	19.84	86.343	12.335		
19	21.07	13.195	2.195		
20	21.97	6.275	0.887		
21	25.13	3.567	0.507		
22	25.40	4.949	0.826		
23	25.97	269.121	47.767	Quercetin	47167.04
24	26.92	7.993	1.718		
25	27.22	3.744	0.672		
26	28.04	3.902	0.610		
27	28.56	5.455	1.044		
28	30.77	1.929	0.352	Kaempferol	269.66
29	31.49	5.300	0.934		
30	31.78	4.748	0.922		
31	34.18	4.150	1.012		

Table 6. HPLC fingerprint Peak table of AP30E

Peak No.	Ret. Time (min)	Height (mAU)	Area (mAU*min)	Name	Amount (mg/kg)
1	3.04	15.913	0.801		
2	3.65	9.274	0.938		
3	4.39	23.988	2.547		
4	4.90	5.122	0.715		
5	6.81	306.654	36.267		
6	8.60	206.386	33.619		
7	9.64	4.111	0.677		
8	11.24	5.679	0.824		
9	11.75	13.052	3.678		
10	12.28	21.860	4.417		
11	12.61	83.357	14.021		
12	13.25	6.336	0.721		
13	14.18	3.273	0.314		
14	15.66	9.698	3.544		
15	16.39	9.118	2.075		
16	17.03	5.047	0.961		
17	17.84	5.627	1.071		
18	18.40	25.966	4.666		
19	19.16	35.664	7.881		
20	19.54	6.879	0.802		
21	19.82	136.835	22.296		
22	21.05	8.670	1.607		
23	21.36	10.462	1.420		
24	21.64	6.921	1.173		
25	21.95	7.135	1.120		
26	22.52	3.798	0.998		
27	22.91	6.635	1.823		
28	23.43	2.743	0.519		
29	23.91	5.836	0.895		
30	25.40	4.780	0.784		
31	25.94	646.549	113.687	Quercetin	112259.82
32	26.92	12.942	2.950		
33	27.21	6.754	1.316		
34	27.57	4.604	1.426		
35	28.53	11.244	2.866		
36	28.78	20.391	4.484		
37	30.43	1.101	0.191		
38	30.75	5.411	1.061	Kaempferol	812.68

39	31.41	49.120	8.516		
40	31.76	14.227	2.567		
41	32.05	12.523	2.154		
42	32.26	15.916	2.669		
43	32.52	6.923	1.642		
44	33.29	7.503	1.566		
45	33.86	10.306	2.514		
46	34.17	19.012	4.973		
47	36.56	26.107	6.882		
48	37.63	5.944	3.020		
49	38.25	2.861	1.214		
50	39.11	3.037	0.500		
51	39.73	2.656	0.524		
52	41.67	14.843	5.823		

Table 7. HPLC fingerprint Peak table of AP50E

Peak No.	Ret. Time (min)	Height (mAU)	Area (mAU*min)	Name	Amount (mg/kg)
1	3.04	19.058	0.982		
2	3.65	8.452	0.810		
3	4.39	10.982	1.257		
4	4.91	4.456	0.727		
5	6.82	199.754	23.483		
6	8.61	91.870	14.635		
7	9.63	5.651	0.896		
8	11.25	4.108	0.555		
9	11.76	12.400	4.513		
10	12.28	28.304	6.187		
11	12.61	162.826	27.980		
12	14.18	3.807	0.549		
13	15.06	3.754	0.671		
14	15.67	8.018	3.678		
15	16.50	9.318	2.971		
16	17.02	5.183	0.837		
17	17.83	4.004	0.862		
18	18.47	13.073	3.199		
19	19.15	30.861	8.127		
20	19.84	105.678	15.352		
21	20.61	3.299	0.536		
22	21.06	4.258	0.507		
23	21.36	8.731	1.212		
24	21.65	4.075	0.730		
25	21.95	5.303	0.844		
26	22.49	6.594	1.628		
27	22.92	6.883	1.661		
28	23.91	27.929	4.357		
29	24.50	15.153	2.307		
30	25.95	567.415	99.767	Quercetin	98514.88
31	27.22	5.530	0.867		
32	27.56	5.677	1.289		
33	28.54	3.687	0.740		
34	28.79	39.585	10.054		
35	29.94	2.957	1.207		
36	30.75	6.442	1.427	Kaempferol	1093.22
37	31.41	89.562	14.772		
38	31.77	16.394	3.039		

39	32.05	28.445	5.288		
40	32.27	22.621	3.732		
41	32.56	25.861	8.338		
42	33.13	38.543	15.264		
43	33.86	21.471	7.514		
44	34.15	20.011	5.541		
45	36.49	110.363	30.359		
46	37.66	15.127	9.316		
47	38.23	13.682	5.990		
48	39.73	6.975	1.346		
49	41.74	57.631	22.290		
50	44.64	19.179	7.395		

DISCUSSION

Inflammatory response is a complex biological mechanism of the immune system that defends the body against injurious stimuli [31]. However, persistent inflammation can lead to uncontrolled chronic inflammation, which can cause many inflammatory diseases and tumorigenesis [32]. Additionally, inflammatory diseases and related immune system disorders are associated with a high prevalence and mortality worldwide [33]. Therefore, maintaining a normal immune status is important to prevent various diseases related to inflammation.

To detect foreign pathogens that cause inflammation, the innate immune system uses pattern recognition receptors (PRRs) encoded by the germline [34]. TLR4, a type of PRRs, is primarily expressed in macrophages and plays an important role in the initiation of inflammation-related immune responses [35]. External pathogens, such as LPS, directly bind to TLR4 on macrophages, resulting in the activation of the macrophages and the elimination of pathogens via phagocytosis [36]. And activated TLR4 signaling pathway induce overactivation of downstream signaling pathways NF-κB and MAPK via myeloid differentiation primary response 88 (MYD88)-dependent signaling and overexpression of pro-inflammatory cytokines [37]. This produced pro-inflammatory mediators act in an

autocrine or paracrine manner on themselves or peripheral immune cells [38]. This positive feedback loop activates various immune cells and promote the production of excessive pro-inflammatory cytokines, which can lead to inflammatory diseases such as systemic inflammatory response syndrome (SIRS), multiple organ failure, and sepsis [39]. Therefore, it is important to prevent continuous activation of immune cells and the secretion of excessive pro-inflammatory mediators for the treatment of inflammation-related diseases.

The JAK-STAT signaling pathway is strongly associated with the induction of inflammation and control of the immune response [40]. Therefore, maintaining pathway homeostasis is important for the immune system of organisms [41, 42]. In an inflammatory environment, pro-inflammatory mediators are excessively produced and distributed, leading to the overactivation of the JAK-STAT pathway; these activated STATs promote the aberrant and excessive expression of pro-inflammatory cytokines in the form of a positive feedback loop, eventually exacerbating inflammatory diseases [43, 44]. It has been studied that JAK2-STAT1 and STAT3 activation promotes a pro-inflammatory responses and STAT3 activation induces unfavorable neuroinflammation in microglia [45, 46]. JAK1/2 inhibitors that reduce activation of JAK1/2 as well as their sub-signals STAT1 and STAT3 have been shown to reduce the expression of inflammatory genes in the inflammatory response induced by α-synuclein in

microglia and macrophages [47]. Therefore, it is important to inhibit JAK-STAT activation during excessive inflammatory response.

Research exploring safe anti-inflammatory materials from various natural products has been actively conducted for a long time, and these studies have recently been applied to various fields such as health foods that can be consumed on daily basis [48]. However, further research on natural products with better anti-inflammatory effects and extraction methods capable of obtaining active ingredients with higher efficiency than natural products is warranted. *A. cepa* is a well-known vegetable with a high flavonoid content, in which the content of quercetin, known for its antioxidant, anti-inflammatory, and anti-cancer effects, is considerably high compared with that in other vegetables [49, 50]. In addition, the flavonoid content, including quercetin, is higher in the peel than in the edible parts of *A. cepa*, however these valuable onion skins are not generally used for human consumption and are either used as feed or discarded [51]. Therefore, studies to confirm the pharmacological effects such as the anti-inflammatory effects of *A. cepa* peel waste are important from the viewpoint of environmental protection and economic feasibility in terms of utilizing waste resources in medicine and research. The anti-inflammatory effects of *A. cepa* peel extracts on LPS-induced HT-29 human colon carcinoma and RAW264.7 cells have been investigated [16, 17]. However, these studies identified the limited effects or mechanisms of *A. cepa* peel extracts using

limited extraction methods. Therefore, in this study, I compared the anti-inflammatory effects of each sample of *A. cepa* peel extracts obtained using various methods and investigated the detailed mechanisms. The most effective extract was identified, and its anti-inflammatory effects and detailed mechanism of AP50E were confirmed in various ways. Our results showed that AP50E had an anti-inflammatory effect in LPS-induced RAW264.7 mouse macrophages by directly inhibiting JAK-STAT signaling. These results suggest therapeutic approaches using AP50E for the inhibition of inflammatory diseases such as atopy, psoriasis, and inflammatory bowel disease, in which macrophages play a pivotal role [4, 52]. However, its anti-inflammatory effects in vivo remain to be determined. Furthermore, since the inflammatory environment, rich in pro-inflammatory mediators, affects the onset and malignancy of cancer, and STATs are highly correlated with poor prognosis of tumors, this also suggests the possibility of approaching AP50E with respect to tumor treatment [53].

In the present study, the anti-inflammatory effects of *A. cepa* peel extracts were investigated using various extraction methods. Among them, AP50E most effectively prevented the production of iNOS, an enzyme related to inflammation and inflammatory mediators such as NO, IL-1α, IL-1β, IL-6 and IL-27. AP50E directly inhibits the JAK-STAT axis, which is associated with inflammation. This study suggests that AP50E can potentially prevent and suppress inflammatory diseases.

REFERENCES

1. Chen, L., et al., Inflammatory responses and inflammation-associated diseases in organs. Oncotarget, 2018. 9(6): p. 7204.
2. Soliman, A.M. and D.R. Barreda, Acute Inflammation in Tissue Healing. International Journal of Molecular Sciences, 2023. 24(1): p. 641.
3. Suzuki, K., Chronic inflammation as an immunological abnormality and effectiveness of exercise. Biomolecules, 2019. 9(6): p. 223.
4. Han, X., et al., Roles of macrophages in the development and treatment of gut inflammation. Frontiers in cell and developmental biology, 2021. 9: p. 625423.
5. Lu, Y.-C., W.-C. Yeh, and P.S. Ohashi, LPS/TLR4 signal transduction pathway. Cytokine, 2008. 42(2): p. 145-151.
6. Banerjee, S., et al., JAK–STAT signaling as a target for inflammatory and autoimmune diseases: current and future prospects. Drugs, 2017. 77: p. 521-546.
7. Malyshev, I. and Y. Malyshev, Current concept and update of the macrophage plasticity concept: intracellular mechanisms of reprogramming and M3 macrophage “switch” phenotype. BioMed research international, 2015. 2015.
8. Yan, Z., et al., Role of the JAK/STAT signaling pathway in regulation of innate immunity in neuroinflammatory diseases. Clinical Immunology, 2018. 189: p. 4-13.

9. Galavi, A., H. Hosseinzadeh, and B.M. Razavi, The effects of Allium cepa L.(onion) and its active constituents on metabolic syndrome: A review. Iranian journal of basic medical sciences, 2021. 24(1): p. 3.
10. Lee, H.-J., et al., Effect of onion extracts on serum cholesterol in borderline hypercholesterolemic participants. Journal of The Korean Society of Food Science and Nutrition, 2010. 39(12): p. 1783-1789.
11. Khajah, M.A., et al., Onion bulb extract reduces colitis severity in mice via modulation of colonic inflammatory pathways and the apoptotic machinery. Journal of ethnopharmacology, 2019. 241: p. 112008.
12. Teshika, J.D., et al., Traditional and modern uses of onion bulb (Allium cepa L.): a systematic review. Critical reviews in food science and nutrition, 2019. 59(sup1): p. S39-S70.
13. Kwak, J.-H., et al., Variation of quercetin glycoside derivatives in three onion (Allium cepa L.) varieties. Saudi Journal of Biological Sciences, 2017. 24(6): p. 1387-1391.
14. Park, S.K., et al., Ameliorating effects of ethyl acetate fraction from onion (Allium cepa L.) flesh and peel in mice following trimethyltin-induced learning and memory impairment. Food Research International, 2015. 75: p. 53-60.
15. Roldán, E., et al., Characterisation of onion (Allium cepa L.) by-products as food ingredients with antioxidant and antibrowning properties. Food Chemistry, 2008. 108(3): p. 907-916.

16. Kim, J., J.-S. Kim, and E. Park, Cytotoxic and anti-inflammatory effects of onion peel extract on lipopolysaccharide stimulated human colon carcinoma cells. Food and chemical toxicology, 2013. 62: p. 199-204.
17. Kang, B.-K., et al., Anti-inflammatory effect of onion (Allium cepa) peel hot water extract in vitro and in vivo. KSBB Journal, 2015. 30(4): p. 148-154.
18. de Bus, I., et al., Immunomodulating effects of 13-and 16-hydroxylated docosahexaenoyl ethanolamide in LPS stimulated RAW264. 7 macrophages. Biochimica et Biophysica Acta (BBA)-Molecular and Cell Biology of Lipids, 2021. 1866(6): p. 158908.
19. Al-Khayri, J.M., et al., Flavonoids as potential anti-inflammatory molecules: A review. Molecules, 2022. 27(9): p. 2901.
20. Lee, H.N., et al., Anti-inflammatory effect of quercetin and galangin in LPS-stimulated RAW264. 7 macrophages and DNCB-induced atopic dermatitis animal models. International Journal of Molecular Medicine, 2018. 41(2): p. 888-898.
21. García-Mediavilla, V., et al., The anti-inflammatory flavones quercetin and kaempferol cause inhibition of inducible nitric oxide synthase, cyclooxygenase-2 and reactive C-protein, and down-regulation of the nuclear factor kappaB pathway in Chang Liver cells. European journal of pharmacology, 2007. 557(2-3): p. 221-229.
22. Lugrin, J., et al., The role of oxidative stress during inflammatory processes. Biological chemistry, 2014. 395(2): p. 203-230.
23. Arulselvan, P., et al., Role of antioxidants and natural products in inflammation. Oxidative medicine and cellular longevity, 2016. 2016.

24. Spychalowicz, A., et al., Novel therapeutic approaches in limiting oxidative stress and inflammation. Current Pharmaceutical Biotechnology, 2012. 13(13): p. 2456-2466.
25. Pi, J., et al., Detection of lipopolysaccharide induced inflammatory responses in RAW264. 7 macrophages using atomic force microscope. Micron, 2014. 65: p. 1-9.
26. Arango Duque, G. and A. Descoteaux, Macrophage cytokines: involvement in immunity and infectious diseases. Frontiers in immunology, 2014. 5: p. 491.
27. Fujiwara, N. and K. Kobayashi, Macrophages in inflammation. Current Drug Targets-Inflammation & Allergy, 2005. 4(3): p. 281-286.
28. He, W., et al., Drug delivery to macrophages: a review of targeting drugs and drug carriers to macrophages for inflammatory diseases. Advanced drug delivery reviews, 2020. 165: p. 15-40.
29. Meka, R.R., et al., IL-27-induced modulation of autoimmunity and its therapeutic potential. Autoimmunity reviews, 2015. 14(12): p. 1131-1141.
30. Di Paolo, N.C. and D.M. Shayakhmetov, Interleukin 1α and the inflammatory process. Nature immunology, 2016. 17(8): p. 906-913.
31. Medzhitov, R., Inflammation 2010: new adventures of an old flame. Cell, 2010. 140(6): p. 771-776.
32. Kiss, A.L., Inflammation in focus: the beginning and the end. Pathology and Oncology Research, 2022: p. 169.
33. Furman, D., et al., Chronic inflammation in the etiology of disease across the life span. Nature medicine, 2019. 25(12): p. 1822-1832.

34. Kawasaki, T. and T. Kawai, Toll-like receptor signaling pathways. Frontiers in immunology, 2014. 5: p. 461.
35. Kuzmich, N.N., et al., TLR4 signaling pathway modulators as potential therapeutics in inflammation and sepsis. Vaccines, 2017. 5(4): p. 34.
36. Zhang, K., et al., Mechanisms of TLR4-mediated autophagy and nitroxidative stress. Frontiers in Cellular and Infection Microbiology, 2021: p. 1026.
37. Rayees, S., et al., Macrophage TLR4 and PAR2 signaling: role in regulating vascular inflammatory injury and repair. Frontiers in Immunology, 2020. 11: p. 2091.
38. Berraondo, P., et al., Cytokines in clinical cancer immunotherapy. British journal of cancer, 2019. 120(1): p. 6-15.
39. Jaffer, U., R. Wade, and T. Gourlay, Cytokines in the systemic inflammatory response syndrome: a review. HSR proceedings in intensive care & cardiovascular anesthesia, 2010. 2(3): p. 161.
40. Malemud, C.J. and E. Pearlman, Targeting JAK/STAT signaling pathway in inflammatory diseases. Current Signal Transduction Therapy, 2009. 4(3): p. 201-221.
41. Xin, P., et al., The role of JAK/STAT signaling pathway and its inhibitors in diseases. International immunopharmacology, 2020. 80: p. 106210.
42. Morales, J., et al., Mast cell homeostasis and the JAK–STAT pathway. Genes & Immunity, 2010. 11(8): p. 599-608.
43. Sabaawy, H.E., et al., JAK/STAT of all trades: linking inflammation with cancer development, tumor progression and therapy resistance. Carcinogenesis, 2021. 42(12): p. 1411-1419.

44. Clark, J.D., M.E. Flanagan, and J.-B. Telliez, Discovery and development of Janus Kinase (JAK) inhibitors for inflammatory diseases: Miniperspective. Journal of medicinal chemistry, 2014. 57(12): p. 5023-5038.
45. Liu, H., et al., Role of Janus kinase/signal transducer and activator of transcription pathway in regulation of expression and inflammation-promoting activity of high mobility group box protein 1 in rat peritoneal macrophages. Shock, 2007. 27(1): p. 55-60.
46. Zheng, Z.V., et al., Novel role of STAT3 in microglia-dependent neuroinflammation after experimental subarachnoid haemorrhage. Stroke and Vascular Neurology, 2022. 7(1): p. 62-70.
47. Qin, H., et al., Inhibition of the JAK/STAT pathway protects against α-synuclein-induced neuroinflammation and dopaminergic neurodegeneration. Journal of Neuroscience, 2016. 36(18): p. 5144-5159.
48. Nunes, C.d.R., et al., Plants as sources of anti-inflammatory agents. Molecules, 2020. 25(16): p. 3726.
49. Sagar, N.A., et al., Onion (Allium cepa L.) bioactives: Chemistry, pharmacotherapeutic functions, and industrial applications. Food Frontiers, 2022. 3(3): p. 380-412.
50. Reyes-Farias, M. and C. Carrasco-Pozo, The anti-cancer effect of quercetin: molecular implications in cancer metabolism. International journal of molecular sciences, 2019. 20(13): p. 3177.
51. Kumar, M., et al., Onion (Allium cepa L.) peel: A review on the extraction of bioactive compounds, its antioxidant potential, and its application as a

functional food ingredient. Journal of Food Science, 2022. 87(10): p. 4289-4311.

52. Kasraie, S. and T. Werfel, Role of macrophages in the pathogenesis of atopic dermatitis. Mediators of inflammation, 2013. 2013.

53. Landskron, G., et al., Chronic inflammation and cytokines in the tumor microenvironment. Journal of immunology research, 2014. 2014.

국문 초록

Allium cepa L. (*A. cepa*) 는 세계에서 가장 오래된 재배 식물 중 하나이다. 또한 식품 및 의약품에 사용되고 염증성 질환을 완화시키는 것으로 알려져 있다. *A. cepa* 껍질은 가식 부위보다 케르세틴과 같은 플라보노이드 함량이 높으며 이는 염증성 질환을 완화하는 효능이 있다. 그러나 여전히 다양한 추출 방법으로 얻은 *A. cepa* 껍질 추출물의 항염증 효과와 그 기본 메커니즘에 관한 연구가 필요하다.

본 연구는 지질다당류 (LPS)가 처리된 RAW264.7 세포에서 다양한 추출 방법으로 정제한 *A. cepa* 껍질 추출물들의 항염증 효능 비교와 관련 세부 메커니즘 규명을 목적으로 하였다. 추출방법이 다른 세 가지 *A. cepa* 껍질 추출물 중 *A. cepa* 껍질 50% EtOH 추출물 (AP50E)이 LPS로 유도된 산화질소 (NO) 및 유도성 산화질소 합성 효소 (iNOS)를 억제하는데 가장 효과적이었다. 또한, AP50E는 전염증성 사이토카인인 인터루킨 (IL)-1α, IL-1β, IL-6 및 IL-27의 수준을 유의하게 감소시켰으며 직접적으로 야누스 키나아제 및 신호변환 및 전사활성인자 (JAK-STAT) 경로를 억제하였다.

이러한 결과는 AP50E가 JAK-STAT 신호를 직접적으로 억제함으로써 LPS로 유도된 RAW264.7 마우스 대식세포에서 항염증 효과를 나타냄을 보여준다. 상기 연구 결과를 바탕으로 AP50E를 염증성 질환에 대한 예방 또는 치료제 개발을 위한 잠재적 후보로 제안할 수 있다.

주요어: *Allium cepa* L., 대식세포, 항염증 효과, 야누스 키아아제 (JAK), 신호변환 및 전사활성인자 (STAT)

학 번: 2021-22420